ADDITIVE MANUFACTURING PROCESS DESIGN

Daniel Clymer*, Jack Beuth*, and Jonathan Cagan*

*Department of Mechanical Engineering, Carnegie Mellon University, Pittsburgh, PA 15213

Abstract

A current issue in metal-based additive manufacturing (AM) is achieving consistent, desired process outcomes in manufactured parts. When process outcomes such as strength, density, or precision need to meet certain specifications, these specifications can be met by changes in process variable selection. However, the changes required to achieve a better part performance may not be intuitive, particularly because process variable changes can simultaneously improve some outcomes while decreasing others. In this work, the tradeoffs between multiple process outcomes are formalized and the design problem is explored throughout the design space of process variables. User input for each process outcome is considered and the best combination of process variables is found to achieve a user's desired outcome.

I. Introduction

Direct metal AM is a rapidly expanding manufacturing method that has found applications within the fields of aerospace, medicine, and others requiring highly complex structures. However, as metal-based AM is a relatively new form of manufacturing, a lack of good process knowledge in the field can cause build results to be more variable than traditional manufacturing methods, thereby limiting its capability. To utilize the full potential of AM as an alternative manufacturing method, it is necessary to have sound understanding about how a part will be affected by its process variable selection. Careful selection of process variables can be a deciding factor in whether a part meets its performance requirements or not, and can greatly improve part quality.

Individual outcomes of the AM process have recently been studied, including microstructure [1], surface finish [2], and residual stresses [3]. Various process variables have been considered, including beam properties [4], scan strategy [5], layer thickness, and particle size [2]. AM processes have been mapped to examine the effect of process variables on melt pool characteristics [1,6]. Much of this current research has given users a better understanding of the available design space in AM, and shown how various process selections can improve properties of interest. In contrast, this study examines the tradeoffs that occur when multiple outcomes are maximized in the same build. In a real design, there are numerous outcomes integral to the product's build and the ability to select process variables that will give balance between all outcomes is greatly desired. The goal in this work is to derive a design method to find the ideal tradeoff in process variables in metal-based AM to deliver the optimal overall part properties.

Often in direct-metal AM, the two most significant process variables are the beam absorbed power (P) and beam travel velocity (V). These variables have the most impact on the rate of heat entering the system, and therefore are the most important for the transient heat

conduction problem. In this research, the behavior of several process outcomes (density, yield strength, surface finish, precision, and deposition rate) is predicted within the P-V design space. Two design methods are discussed: one method based on user preference for multiple outcomes that finds optimal processing directions for the user's case, and one method based on user requirement for each outcome that finds regions of P-V space satisfying the user requirements. As is outlined in several case studies, these results can direct the user to a choice of beam power and velocity that are different than the machine nominal settings, resulting in a better part. Applying process mapping techniques to the P-V design space allows the user to achieve a better set of process outcomes for a given design consideration.

II. Methods

The desired result of this study is to find the best process variable combination based on a user's input for a number of process outcomes. The process outcomes included in the study are: density, yield strength, surface finish, precision, and deposition rate. These have been included because they are outcomes that are often considered important to part designers. The process variables are absorbed power (P) and beam scanning velocity (V). Through a number of basic assumptions about the AM process, each outcome is tied back to these two process variables, and equations are created that show how each outcome is expected to change throughout P-V space. The outcomes are calculated for type 316L stainless steel, although most of the trends discussed would be similar in other materials as well.

1. Assumptions

In order to reduce the process variables down to two (beam power and beam velocity), a series of assumptions about other important process variables were made.

a.) Hatch Spacing and Layer Thickness – The layer thickness (thickness of the new powder layer) and hatch spacing (the distance between the centers of the deposited beads) are variables that can be changed on the machine. However, both variables will typically scale with the melt pool size. This is because the layer thickness and hatch spacing need to be smaller than the melt pool depth and width, respectively, in order for all material to be fully melted. Once a factor of safety is chosen (say, 50% of the melt pool depth), good choices for the layer thickness and hatch spacing can be determined by the melt pool size.

b.) Powder Size – The powder size distribution is known to affect the surface quality of the resulting part [2]. One constraint on powder size is that it cannot have bigger particles than the size of the melt pool, or else some material would not be melted. The other factor to consider is the drastic increase in cost as smaller particle size distributions are used. This means that it is typically much more economical to use the biggest particle size distribution possible for a given melt pool size. Thus, particle size can be bounded above and below by melt pool size.

2. Melt Pool Calculations

In order to calculate the process outcomes, the melt pool sizes must be predicted throughout P-V space. Finite element simulations, modeling the laser powder process, were run using ABAQUS software, and predicted melt pool quantities throughout P-V space. This model was similar to the model created by Soylemez [14], or more recently, Montgomery [15], but for stainless steel. The model simulated a distributed heat source scanning over a substrate of

stainless steel 316L. The other surfaces in the model were maintained at a boundary condition temperature corresponding to the preheat temperature of the process, 373 K. A symmetric boundary condition was imposed on the mid-plane to reduce computation time. Melt pool properties were calculated for six P-V combinations, which were: 50W-200mm/s, 50W-500mm/s, 50W-1400mm/s, 200W-200mm/s, 200W-500mm/s, 200W-1400mm/s. These 6 points can be used to map out P-V space in terms of the melt pool characteristics. This type of mapping has been observed to closely follow the real behavior throughout P-V space of a direct metal AM-produced material [14]. All of the calculations in the research are done for stainless steel type 316L.

3. Process Outcome Calculations

The process outcomes considered in this study were: density, yield strength, surface roughness, precision, and deposition rate. Curves for each of these outcomes were tied back to the experimental results found for type 316L stainless steel.

a) **Porosity and Susceptibility to Flaws** – Achieving full density is typically one of the most important requirements for an additively manufactured part. The likelihood of porosity is related to how much overlap there is between the scanning melt pool and the top of the previous layer. Note that because the powder layer will shrink by as much as 55% when it is melted [10], the effective layer thickness (the thickness of powder the melt pool has to melt through) will be larger than the actual resulting layer thickness.

Spierings et al [11] found a correlation between the energy density supplied to the powder layer and the resulting density of the part. The energy density, given in Eq. (1) takes laser power, velocity, hatch spacing, and layer thickness into account.

$$E - Density = \frac{P}{v \times h \times t_{layer}} \ . \tag{1}$$

The approximate relationship to energy density is given in Eq. (2),

$$Density = 0.92 + 12.2a - 514a^2 + 4318a^3, \tag{2}$$

where h is the hatch spacing, t is the layer thickness, and a=1/E-Density. With lower energy density, more flaws are likely to develop in the part. Note the dependence on hatch spacing and layer thickness: changing these can help fix porosity problems even with low power settings.

b) **Yield Strength** – Additively manufactured austenitic stainless steel has been observed to form a fine microstructure, due to the high cooling rates characteristic of the AM process [12–15]. Although a detailed model has not been created to describe yield strength dependence in processing space, it has been shown that this microstructure gets finer with faster characteristic cooling rates, and that the strength increases with these finer microstructures [14,16]. Because a detailed model governing strength throughout processing space has not been found thus far, this research assumed a Hall-Petch relationship, which says that there is an inverse relationship between yield strength and grain size in a material. This type of relationship occurs because moving dislocations, which cause eventual yield in the material, are impeded at the grain boundaries. This makes materials with smaller grains (more grain boundaries) stop dislocation movement better and therefore take more applied stress before yielding. The well-known Hall-Petch equation is given in Eq. (3):

$$\sigma = \sigma_0 + K_H d^{-1/2}, \tag{3}$$

where σ is the yield strength, d is the grain size, and σ_o and K_H are constants.

c) **Surface Finish** – Surface finish is typically defined in terms of Ra, which is the average of the absolute value of the profile height deviations from the mean height of a surface [17]. Spierings et. al [2] showed that the as-built Ra of an AM part scales with the average particle size of the powder in metal-based AM. Assuming a linear scaling (we expect particles half the size to have half the Ra value), the expected trend can be predicted throughout P-V space. The equation used for surface finish is given in Eq. (4):

$$SF = C \times D, \tag{4}$$

where SF is the surface finish, D is the average particle diameter, and C is a constant depending on material.

d) **Precision** – The obtainable precision refers to the smallest feature that the machine is able to reliably deposit during the build. This value scales with the average melt pool width, because the process is only capable of creating features that are bigger than one of the melt pools [18]. The equation used to govern precision changes throughout the domain is given in Eq. (5):

$$P = C \times MPW, \tag{5}$$

where P is the precision, MPW is the melt pool width, and C is a constant.

e) **Deposition Rate** – The deposition rate is the rate at which new melted material is being added to the part. Eq. (6) gives the equation used to calculate deposition rate:

$$DR = t \times h \times v, \tag{6}$$

where t is the layer thickness, h is the hatch spacing (distance between the center of two beads), and v is beam scanning velocity. As discussed in the assumptions section, the layer thickness and hatch spacing should also scale with melt pool size, which can relate the deposition rate back to the melt pool size and ultimately to the power and velocity settings.

III. Results

1. Design Tool #1: Weighted-Sum Method

As discussed in section I, the weighted-sum method reduces the multiple objectives (density, yield strength, surface roughness, precision, and deposition rate) down to one objective by a weighted summation of each objective. Because of the differing ranges in process outcomes, each outcome was normalized to have a maximum value of one and a minimum value of 0 in the range of P-V space. The weights were determined by user preference for each outcome, with a user input between 0-10, with 10 being the most important. The resulting weighted-sum objective function was mapped out as a contour plot in P-V space.

a. Weighted Sum Method: Case Study

In an example using the weighted-sum design tool, consider user preferences weighting yield strength and deposition rate highly. The weightings are given in Table 2, and the contour map of the weighted-sum objective function is shown in Figure 7.
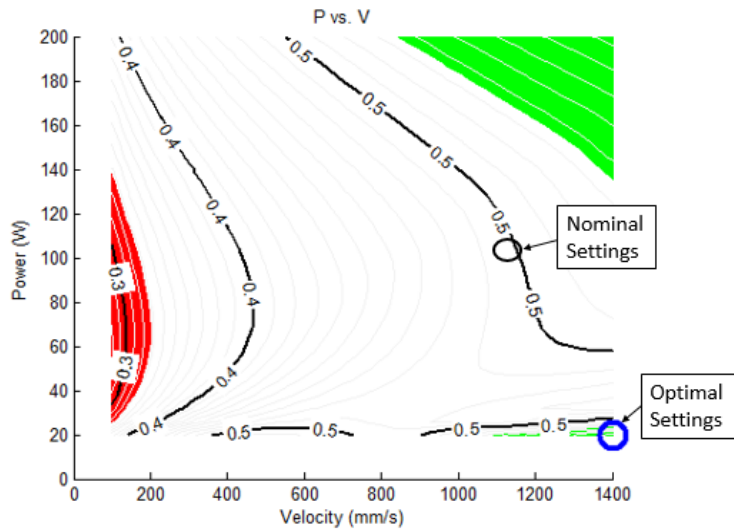
Figure 1: Weighted-Sum contour plot in P-V space for the weighted-sum case study #2

Table 2: Weighted Sum Case Study Requirements

Outcome	User Weighting
Density	3
Yield Strength	7
Surface Roughness	1
Precision	3
Build Rate	5

Figure 7 shows two regions of higher contour values, both the upper right and lower right regions of P-V space. In this case, the user could make process improvements by making a move in either direction in P-V space.

2. Design Tool #2: Bounded Objective Method

The second design tool explored in this study took user requirement for all but one process outcome and found a "processing window" in P-V space that satisfied each of these requirements. Within the processing window, the final outcome was optimized to direct the user to the best P-V combination within the window.

a. Bounded Objective Method: Case Study

As an example, consider a part that will have small features, requiring tight precision tolerance, as well as a tight regulation on part density. For illustration, requirements are shown in Table 3. After meeting each of these requirements, it is desired to maximize the build rate. Figure 8 shows a contour plot of build rate in P-V space, overlaid with each constraint requirement. The green (shaded) region shows the area that satisfies all build requirements. In this case, the yield strength constraint is active. The optimum within that region is in the upper right, where the build rate is maximized.
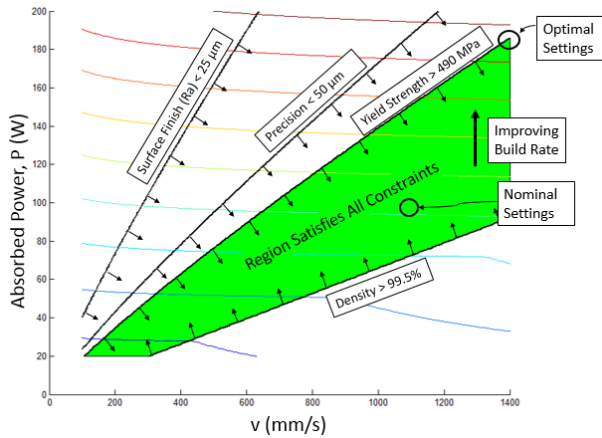
Figure 2: Case Study #1, showing objective contours of build rate overlaid on design constraint requirements

Table 3: Bounded Objective Case Study #1 Requirements

Surface Finish (Ra)	Less Than 25 μm
Precision	Less Than 50 μm
Density	Above 99.5%
Yield Strength	Greater Than 490 MPa
Maximize Build Rate	

A designer for additive manufacturing could use this information to alter the process input variables to achieve a part more closely aligned with their required output. In this example, the optimal P-V combination that was found is: P = 186 W, V = 1400 mm/s. This deviates from the machine nominal settings for 316L stainless steel, which are P = 98 W, V = 1083 mm/s. They can also use this to have feedback on which constraints, if relaxed somewhat, would change the optimal solution, and which would not affect the optimum. In this example, relaxing the constraint on yield strength would change the location of the optimum.

IV. Discussion

This study explored two methods of assisting an AM user in finding the best regions of P-V operating space: one method using a weighted summation of objectives, and one method using a bounded objective function method. The first can be used to show the user the best direction to move in processing space by finding the direction of the steepest gradient change. The second can be used in situations that the user has more knowledge of specific outcome requirements, to show the user a "processing window" that satisfies all requirements. Typically, the suggested processing variables will show that a deviation from the nominal machine settings provides a build result more closely aligned with the desired outcomes.

In the case study involving the weighted-sum objective function, the P-V contour map showed the best regions for the user's preference in process outcomes. One of the most important uses for this kind of contour map is to show the user the optimal direction to move away from the nominal settings in processing space. This is especially useful for AM users that have a limited understanding of how important process outcomes will change in P-V space, and want to have an idea of what parameter changes will benefit their goals before investing in time-consuming and costly experiments on the machine.

In the case study involving the bounded objective function, the results suggested a deviation away from the machine nominal settings, which for these examples is P = 98 W, V = 1083 mm/s. This demonstrates the fact that these process variables can be tailored for each specific situation, to create better design outcomes than would have resulted from the nominal settings, depending on user requirement for that situation. These examples also demonstrated the concept of a "processing window" that the user could operate within to satisfy their process

requirements. This kind of design tool is useful for more experienced AM users that know exactly what requirements they need to meet in order to have a successful part.

In many cases, the machine nominal settings will fall inside this "processing window". This is because the nominal settings were likely selected to achieve a decent result for a wide range of requirements. However, for specific situations, these nominal settings will not necessarily be the best choice of process variables. A process that is designed with user requirement in mind, that varies from case to case, can achieve better outcomes for each case than a machine operating nominally.

Because additive manufacturing is such a new technology, coupled with the fact that most users do not deviate from the nominal process variables, much work still needs to be done to characterize different AM processes and materials. In this work, general expected trends are used as an example to show how a designer might formulate the problem of process design. It is expected that experimental results would yield somewhat different values, compared to the predictions in this study, but the trends are expected to be similar. In the future, it will be of great use to the designer to have more comprehensive experiments characterizing all of the design space.

V. Conclusions

One of the most appealing aspects of additive manufacturing is the ability for builds to be customized specifically to a user's application. Applying process mapping techniques to the P-V design space in additive manufacturing has produced insight into how an AM user might approach the selection of process variables. This study demonstrates an opportunity to design the process of additive manufacturing to achieve a set of outcomes tailored to the user's needs. A real part will typically have multiple process outcome that need to be simultaneously improved. In AM, these outcomes often depend on the same input variables, making tradeoffs between design outcomes a necessity. Based off of user preference or requirement, design variables can be altered to reach the best combination of process outcomes achievable for a user's application.

In the future, as more research is done to improve the field's understanding of process outcomes' relationship to process variables in AM, the assumptions made in this paper will be refined to give more precise results. Additional process variables and processes could be incorporated into the algorithm, resulting in more freedom to the process designer to build an optimal part. As knowledge of process outcomes becomes more detailed and can be predicted with more accuracy, additive manufacturing processes will be designed for greater user customization.

References

[1]   Gockel, J., and Beuth, J., 2013, "Understanding Ti-6Al-4V Microstructure Control in Additive Manufacturing via Process Maps," Solid Freeform Fabrication Proceedings, pp. 666–674.

[2]   Spierings, A. B., Herres, N., Levy, G., and Buchs, C., 2011, "Influence of the particle size distribution on surface quality and mechanical properties in additive manufactured stainless steel parts," Rapid Prototyp. J., **17**(3), pp. 195–202.

[3]   Peter Mercelis, J. K., 2006, "Residual stresses in selective laser sintering and selective laser melting," Rapid Prototyp. J., **12**(5), pp. 254–265.

[4]   Murr, L., Martinez, E., Medina, F., Gaytan, S. M., Ramirez, D. A., Hernandez, J., Amato, K. N., Shindo, P. W., and Wicker, R. B., 2012, "Metal Fabrication by Additive Manufacturing Using Laser and Electron Beam Melting Technologies," J. Mater. Sci. Technol., **28**(1), pp. 1–14.

[5]   Mertens, R., Clijsters, S., Kempen, K., and Kruth, J.-P., 2014, "Optimization of Scan Strategies in Selective Laser Melting of Aluminum Parts With Downfacing Areas," J. Manuf. Sci. Eng., **136**(December 2014).

[6]   Beuth, J., Fox, J., Gockel, J., Montgomery, C., Yang, R., Qiao, H., Reeseewatt, P., Anvari, A., Narra, S., and Klingbeil, N., 2013, "Process Mapping for Qualification Across Multiple Direct Metal Additive Manufacturing Processes," Solid Freeform Fabrication Proceedings, pp. 655–665.

[7]   Marler, R. T., and Arora, J. S., 2004, "Survey of multi-objective optimization methods for engineering," Struct. Multidisc. Optim., **26**, pp. 369–395.

[8]   Kruth, J., Badrossamay, M., Yasa, E., Deckers, J., Thijs, L., and Humbeeck, J. Van, 2010, "Part and material properties in selective laser melting of metals," 16th International Symposium on Electromachining, pp. 1–12.

[9]   Lima, M. S. F. de, and Sankare, S., 2014, "Microstructure and mechanical behavior of laser additive manufactured AISI 316 stainless steel stringers," Mater. Des., (March), pp. 526–532.

[10]   Yu, J., Rombouts, M., and Maes, G., 2013, "Cracking behavior and mechanical properties of austenitic stainless steel parts produced by laser metal deposition," Mater. Des., **45**, pp. 228–235.

[11]   Fu, J. W., Yang, Y. S., Guo, J. J., and Tong, W. H., 2008, "Effect of cooling rate on solidification microstructures in AISI 304 stainless steel," Mater. Sci. Technol., **24**(8), pp. 941–944.

[12]   Wang, Z., Palmer, T. A., and Beese, A. M., 2016, "Effect of processing parameters on microstructure and tensile properties of austenitic stainless steel 304L made by directed energy deposition additive manufacturing," Acta Mater., **110**, pp. 226–235.

[13]   Smugeresky, J. E., Keicher, D. M., Romero, J. A., Griffith, M. L., and Harwell, L. D., 1997, Laser Engineered Net Shaping (LENSTM) Process : Optimization of Surface Finish and Microstructural Properties, Albuquerque, NM.

[14] Beuth, J., Soylemez, E., and Taminger, K., 2010, "Controlling melt pool dimensions over a wide range of material deposition rates in electron beam additive manufacturing," Solid Freeform Fabrication Proceedings, pp. 571–582.

[15] Montgomery, C., Beuth, J., Sheridan, L., and Klingbeil, N., 2015, "Process Mapping of Inconel 625 in Laser Powder Bed Additive Manufacturing," Solid Freeform Fabrication, pp. 1195–1204.

[16] Yasa, E., and Kruth, J., 2012, "Microstructural investigation of Selective Laser Melting 316L stainless steel parts exposed to laser re-melting," 1st CIRP Conference on Surface Integrity, pp. 389–395.

[17] Steen, W. M., and Mazumder, J., 2010, Laser Materials Processing, Springer, London.

[18] A.B. Spierings, K. Wegener, G. L., 2012, "Designing Material Properties Locally with Additive Manufacturing technology SLM," Solid Freeform Fabrication, pp. 447–455.

[19] Guo, W., and Kar, A., 1999, "Prediction of microstructures in laser welding of stainless steel AISI 304," J. Laser Appl., **11**(4), pp. 185–189.

[20] Whitehouse, D., 2012, Surfaces and their Measurement, Butterworth-Heinemann, Boston.

[21] Adam, G. A. O., and Zimmer, D., 2014, "Design for Additive Manufacturing — Element transitions and aggregated structures," CIRP J. Manuf. Sci. Technol., **7**, pp. 20–28.